Electronic Supplementary Material (ESI) for Journal of Materials Chemistry A.

Supporting Information

Cu single-atom on Ti_2CO_2 as high efficient oxygen reduction catalyst in proton exchange membrane fuel cell

Qiong Peng, Jian Zhou*, Jiatian Chen, Tian Zhang, Zhimei Sun*

School of Materials Science and Engineering, Beihang University, Beijing 100191, China

Center for Integrated Computational Materials Engineering, International Research Institute for Multidisciplinary Science, Beihang University, Beijing 100191, China

*Corresponding Authors: jzhou@buaa.edu.cn (Jian Zhou), zmsun@buaa.edu.cn (Zhimei Sun)

Calculation details for adsorption free energy and reaction free energy

In proton exchange membrane fuel cell, the cathode is a place for O_2 reduction, where the overall reaction is: $O_2(g) + 4H^+ + 4e^- \rightarrow 2H_2O$, composed of four elementary steps:

$$O_2(g) + H^+ + e^- + * \rightarrow *OOH, \quad (1)$$

$$*OOH + H^+ + e^- \rightarrow *O + H_2O(l), \quad (2)$$

$$*O + H^+ + e^- \rightarrow *OH, \quad (3)$$

$$*OH + H^+ + e^- \rightarrow H_2O(l) + *, \quad (4)$$

where * is the active site on the catalytic surface. (g) and (l) correspond to the gap and liquid phases, respectively. According to the reversible hydrogen electrode (RHE) model proposed by Nørskov et al,[1] the chemical potential (μ) of a proton-electron pair is equivalent to that of half a H_2 molecule: $\mu_{H^+} + \mu_{e^-} = 0.5\mu_{H_2}$, at U= 0 V and P_{H2}= 1 bar. Based on the definition of chemical potential $\mu = E + \mathrm{ZPE} - T \times S$ (E is the total energy achieved from DFT calculations, ZPE is zero-point energy and S is the entropy at 298 K), the adsorption free energy of the ORR intermediates (ΔG_{*OOH}, ΔG_{O*} and ΔG_{*OH}) are derived from the following formulas,

$$\Delta G_{*OOH} = \Delta G(2H_2O(g) + * \rightarrow *OOH + 1.5H_2(g)) = \mu_{*OOH} + 1.5\mu_{H_2} - 2\mu_{H_2O} - \mu_*$$

$$= (E_{*OOH} + 1.5 \times E_{H_2} - 2 \times E_{H_2O} - E_*) + (\mathrm{ZPE}_{*OOH} + 1.5 \times \mathrm{ZPE}_{H_2} - 2 \times \mathrm{ZPE}_{H_2O} - \mathrm{ZPE}_*)$$

$$-T \times (S_{*OOH} + 1.5 \times S_{H_2} - 2 \times S_{H_2O} - S_*) \quad (5)$$

$$\Delta G_{O*} = \Delta G(H_2O(g) + * \rightarrow O* + H_2(g)) = \mu_{O*} + \mu_{H_2} - \mu_{H_2O} - \mu_*$$

$$= (E_{O*} + E_{H_2} - E_{H_2O} - E_*) + (\mathrm{ZPE}_{O*} + \mathrm{ZPE}_{H_2} - \mathrm{ZPE}_{H_2O} - \mathrm{ZPE}_*) - T \times (S_{O*} + S_{H_2} - S_{H_2O} - S_*) \quad (6)$$

$$\Delta G_{*OH} = \Delta G(H_2O(g) + * \rightarrow *OH + 0.5H_2(g)) = \mu_{*OH} + 0.5\mu_{H_2} - \mu_{H_2O} - \mu_*$$

$$= (E_{*OH} + 0.5 \times E_{H_2} - E_{H_2O} - E_*) + (\mathrm{ZPE}_{*OH} + 0.5 \times \mathrm{ZPE}_{H_2} - \mathrm{ZPE}_{H_2O} - \mathrm{ZPE}_*)$$

$$-T\times(S_{*\mathrm{OH}}+0.5\times S_{\mathrm{H_2}}-S_{\mathrm{H_2O}}-S_{*}) \quad (7)$$

The ZPE for each adsorbate and gaseous molecules can be obtained from the vibration frequency calculation, while the ZPE of substrates is negligible. Notably, for the same adsorbate on different supports, the ZPE shows the same value since they have rather close value.[2] Entropy results of free molecules are taken the standard thermodynamic tables,[3] while the entropies of adsorbate and substrate are negligible. All the ZPE and entropy values are summarized in Table S1. In formulas (5-7), gas-phase H_2O and H_2 were used as reference states because they are readily treated in the DFT calculations. In contrast, the high-spin ground state of O_2 is poorly described in DFT calculations, thus the free energy of the O_2(g) was derived based on the equation of $G_{\mathrm{O_2(g)}}=2G_{\mathrm{H_2O(l)}}-2G_{\mathrm{H_2}}+4.92$ eV.[4] The free energy of OH^- was obtained by $G_{\mathrm{OH^-}}=G_{\mathrm{H_2O(l)}}-G_{\mathrm{H^+}}$. The free energy for gas phase H_2O(g) is calculated at 0.035 bars because this is the equilibrium pressure of H_2O at 298 K. The free energy of this state is equal to that of liquid H_2O(l).

The reaction free energy from initial state to final state is defined as:

$$\Delta G = \Delta E + \Delta\mathrm{ZPE} - \mathrm{T}\Delta S + \Delta G_{\mathrm{pH}} + \Delta G_U, \quad (8)$$

where ΔE is the total energy change achieved from DFT calculations. ΔZPE and ΔS are the change in zero-point energy and entropy owing to the reaction, respectively. $\Delta G_{\mathrm{pH}} = -k_{\mathrm{B}}T\ \ln[\mathrm{H^+}] = \mathrm{pH}\times k_{\mathrm{B}}T\ \ln10$, owing to the effect of pH value of the electrolyte. The bias effect on the free energy $\Delta G_{\mathrm{U}} = -neU$, where U is the applied electrode potential, e is the transferred charge, and n is the number of proton−electron transferred pairs. Eventually, for each ORR elementary step in equation (1-4), the reaction free energy (ΔG_1, ΔG_2, ΔG_3 and ΔG_4) is derived as:

$$\begin{aligned}\Delta G_1 &= \mu_{*\mathrm{OOH}}+\mu_{\mathrm{OH^-}}-\mu_{\mathrm{H_2O}}-\mu_{*}-\mu_{\mathrm{O_2}}-\mu_{\mathrm{e^-}}\\ &= \mu_{*\mathrm{OOH}}+(\mu_{\mathrm{H_2O}}-\mu_{\mathrm{H^+}})-\mu_{\mathrm{H_2O}}-\mu_{*}-(2\mu_{\mathrm{H_2O}}-2\mu_{\mathrm{H_2}}+4\times1.23)-\mu_{\mathrm{e^-}}\end{aligned}$$

$$= \mu_{*OOH} + 1.5\mu_{H_2} - 2\mu_{H_2O} - \mu_* - 4.92$$

$$= \Delta G_{*OOH} - 4.92 \quad (9)$$

$$\Delta G_2 = \mu_{O*} + \mu_{OH^-} - \mu_{*OOH} - \mu_{e^-}$$

$$= \mu_{O*} + (\mu_{H_2O} - \mu_{H^+}) - \mu_{*OOH} - \mu_{e^-}$$

$$= \mu_{O*} + \mu_{H_2O} - 0.5\mu_{H_2} - \mu_{*OOH}$$

$$= (\mu_{O*} + \mu_{H_2} - \mu_{H_2O} - \mu_*) - (\mu_{*OOH} + 1.5\mu_{H_2} - 2\mu_{H_2O} - \mu_*)$$

$$= \Delta G_{O*} - \Delta G_{*OOH} \quad (10)$$

$$\Delta G_3 = \mu_{*OH} + \mu_{OH^-} - \mu_{O*} - \mu_{H_2O} - \mu_{e^-}$$

$$= \mu_{*OH} + (\mu_{H_2O} - \mu_{H^+}) - \mu_{O*} - \mu_{H_2O} - \mu_{e^-}$$

$$= \mu_{*OH} - 0.5\mu_{H_2} - \mu_{O*}$$

$$= (\mu_{*OH} + 0.5\mu_{H_2} - \mu_{H_2O} - \mu_*) - (\mu_{O*} + \mu_{H_2} - \mu_{H_2O} - \mu_*)$$

$$= \Delta G_{*OH} - \Delta G_{O*} \quad (11)$$

$$\Delta G_4 = \mu_{OH^-} + \mu_* - \mu_{*OH} - \mu_{e^-}$$

$$= (\mu_{H_2O} - \mu_{H^+}) + \mu_* - \mu_{*OH} - \mu_{e^-}$$

$$= \mu_{H_2O} - 0.5\mu_{H_2} + \mu_* - \mu_{*OH}$$

$$= -(\mu_{*OH} + 0.5\mu_{H_2} - \mu_{H_2O} - \mu_*)$$

$$= -\Delta G_{*OH} \quad (12)$$

Tables

Table S1. Values used of the DFT total energy (E_{tot}), zero-point energy (ZPE) corrections and entropic contribution (TS, T = 298.15 K) to the free energy. For the same adsorbate, the ZPE takes the same value since they have rather close value even on different substrates. Entropy values of free molecules are taken from the standard thermodynamic tables, while the entropies of adsorbate and substrate are negligible.

Species	E_{tot} (eV)	ZPE (eV)	TS (eV)
H_2O	-14.22	0.57	0.67
H_2	-6.77	0.27	0.40
O_2	-9.86	0.10	0.63
O_2*	-	0.16	0
O*	-	0.07	0
OH*	-	0.36	0
OOH*	-	0.42	0

Table S2. The valence electrons ($\varphi_M^{anchored}$) and electronegativity ($\chi_M^{anchored}$) of 3d, 4d and 5d transition-metals as well as the electronegativity (χ) of O, C and N atoms.

atom	$\varphi_M^{anchored}$	$\chi_M^{anchored}$	atom	$\varphi_M^{anchored}$	$\chi_M^{anchored}$	atom	$\varphi_M^{anchored}$	$\chi_M^{anchored}$	atom	χ
Ti	4	1.54	Zr	4	1.33	Hf	4	1.32	O	3.44
V	5	1.63	Nb	5	1.59	Ta	5	1.51	C	2.55
Cr	6	1.66	Mo	6	2.16	W	6	2.36	N	3.04
Mn	7	1.55	Tc	7	1.91	Re	7	1.93		
Fe	8	1.83	Ru	8	2.20	Os	8	2.18		
Co	9	1.88	Rh	9	2.28	Ir	9	2.20		
Ni	10	1.92	Pd	10	2.20	Pt	10	2.28		
Cu	11	1.90	Ag	11	1.93	Au	11	2.54		

Table S3. Adsorption free energies of O* (ΔG_{O*}, eV), *OH (ΔG_{*OH}, eV) and *OOH (ΔG_{*OOH}, eV) reaction intermediates as well as the composition descriptor $\xi = \varphi_M^{anchored} \times \chi_O^{ads} / (\chi_M^{anchored} + \chi^{MXene})$ on M-Ti_2CO_2 (M = 3d, 4d and 5d transition-metal).

Active center	ξ	ΔG_{O*}	ΔG_{*OH}	ΔG_{*OOH}
Ti-Ti_2CO_2	3.40	-1.29	-1.78	1.57
V-Ti_2CO_2	4.16	-1.36	-1.11	2.36
Cr-Ti_2CO_2	4.96	-1.09	-0.80	2.30
Mn-Ti_2CO_2	5.94	0.88	0.89	3.84
Fe-Ti_2CO_2	6.35	1.41	0.00	3.31
Co-Ti_2CO_2	7.07	1.39	0.24	3.39
Ni-Ti_2CO_2	7.78	2.09	0.97	3.83
Cu-Ti_2CO_2	8.60	2.78	1.25	3.76
Zr-Ti_2CO_2	3.59	-1.37	-2.33	1.55
Nb-Ti_2CO_2	4.20	-1.94	-1.66	1.95
Mo-Ti_2CO_2	4.43	-1.51	-0.68	1.88
Tc-Ti_2CO_2	5.46	-1.10	-0.50	2.33
Ru-Ti_2CO_2	5.85	0.60	0.76	3.45
Rh-Ti_2CO_2	6.47	1.68	0.81	3.68
Pd-Ti_2CO_2	7.32	2.80	1.81	4.05
Ag-Ti_2CO_2	8.54	3.60	1.79	4.37
Hf-Ti_2CO_2	3.60	-1.19	-2.54	1.35
Ta-Ti_2CO_2	4.29	-2.44	-2.26	1.53
W-Ti_2CO_2	4.25	-1.87	-1.06	1.77
Re-Ti_2CO_2	5.43	-1.39	-0.72	2.01
Os-Ti_2CO_2	5.88	-0.56	0.28	2.79
Ir-Ti_2CO_2	6.58	0.65	0.48	2.90
Pt-Ti_2CO_2	7.19	1.53	1.26	3.24
Au-Ti_2CO_2	7.50	2.69	1.68	3.14

Table S4. Adsorption free energies of O* (ΔG_{O*}, eV), *OH (ΔG_{*OH}, eV) and *OOH (ΔG_{*OOH}, eV) reaction intermediates as well as the composition descriptor $\xi = \varphi_M^{anchored} \times \chi_O^{ads} / (\chi_M^{anchored} + \chi^{MXene})$ on M-$Ti_3C_2O_2$ (M = 3d, 4d and 5d transition-metal).

Active center	ξ	ΔG_{O*}	ΔG_{*OH}	ΔG_{*OOH}
Ti-$Ti_3C_2O_2$	3.52	-1.14	-1.86	1.79
V-$Ti_3C_2O_2$	4.30	-1.41	-1.25	1.81
Cr-$Ti_3C_2O_2$	5.12	-0.87	-0.14	2.37
Mn-Ti3C_2O_2	6.14	1.08	0.93	3.89
Fe-$Ti_3C_2O_2$	6.55	1.26	-0.20	3.12
Co-$Ti_3C_2O_2$	7.28	1.60	0.45	3.56
Ni-$Ti_3C_2O_2$	8.02	1.90	0.70	3.73
Cu-$Ti_3C_2O_2$	8.86	2.79	1.42	3.72
Zr-$Ti_3C_2O_2$	3.72	-1.18	-2.30	1.09
Nb-$Ti_3C_2O_2$	4.34	-2.12	-1.78	1.65
Mo-$Ti_3C_2O_2$	4.55	-1.77	-0.95	1.53
Tc-$Ti_3C_2O_2$	5.62	-1.11	-0.29	2.20
Ru-$Ti_3C_2O_2$	6.02	0.18	0.59	3.03
Rh-$Ti_3C_2O_2$	6.66	1.70	1.01	3.90
Pd-$Ti_3C_2O_2$	7.53	2.59	1.95	3.91
Ag-$Ti_3C_2O_2$	8.80	3.79	2.00	4.34
Hf-$Ti_3C_2O_2$	3.73	-0.96	-2.55	0.89
Ta-Ti_3C_2O2	4.43	-2.46	-2.38	1.44
W-$Ti_3C_2O_2$	4.36	-2.27	-1.28	1.12
Re-$Ti_3C_2O_2$	5.60	-1.38	-0.54	1.93
Os-$Ti_3C_2O_2$	6.05	-0.79	-0.08	2.48
Ir-$Ti_3C_2O_2$	6.77	0.51	0.85	2.93
Pt-$Ti_3C_2O_2$	7.40	1.44	0.94	3.04
Au-$Ti_3C_2O_2$	7.70	2.69	1.71	3.12

Table S5. Adsorption free energies of O* (ΔG_{O*}, eV), *OH (ΔG_{*OH}, eV) and *OOH (ΔG_{*OOH}, eV) reaction intermediates as well as the composition descriptor $\xi = \varphi_M^{anchored} \times \chi_O^{ads} / (\chi_M^{anchored} + \chi^{MXene})$ on M-Ti_3CNO_2 (M = 3d, 4d and 5d transition-metal).

Active center	ξ	ΔG_{O*}	ΔG_{*OH}	ΔG_{*OOH}
Ti-Ti_3CNO_2	3.46	-1.24	-1.89	1.76
V-Ti_3CNO_2	4.22	-1.56	-1.22	2.20
Cr-Ti_3CNO_2	5.03	-0.87	-0.64	2.52
Mn-Ti_3CNO_2	6.03	1.14	0.08	4.07
Fe-Ti_3CNO_2	6.44	1.50	-0.25	3.10
Co-Ti_3CNO_2	7.16	1.52	0.38	3.48
Ni-Ti_3CNO_2	7.89	1.83	0.62	3.64
Cu-Ti_3CNO_2	8.72	2.81	1.30	3.76
Zr-Ti_3CNO_2	3.65	-1.28	-2.34	1.04
Nb-Ti_3CNO_2	4.27	-2.20	-1.95	1.72
Mo-Ti_3CNO_2	4.49	-1.93	-1.10	1.39
Tc-Ti_3CNO_2	5.53	-1.14	-0.28	2.22
Ru-Ti_3CNO_2	5.93	0.10	0.70	3.04
Rh-Ti_3CNO_2	6.56	1.62	0.98	3.95
Pd-Ti_3CNO_2	7.41	2.50	1.64	3.81
Ag-Ti_3CNO_2	8.66	3.76	1.96	4.50
Hf-Ti_3CNO_2	3.66	-1.04	-2.57	0.84
Ta-Ti_3CNO_2	4.35	-2.49	-2.49	1.00
W-Ti_3CNO_2	4.30	-2.41	-1.43	0.87
Re-Ti_3CNO_2	5.51	-1.43	-0.51	1.90
Os-Ti_3CNO_2	5.95	-0.79	0.13	2.50
Ir-Ti_3CNO_2	6.67	0.33	0.60	2.78
Pt-Ti_3CNO_2	7.29	1.33	0.81	2.88
Au-Ti_3CNO_2	7.60	2.66	1.70	3.17

Table S6. O* adsorption free energy (ΔG_{O*}, eV) of previously reported ORR catalysts possessing comparable or even better catalytic activity compared to commercial Pt/C.

system	ΔG_{O*}	References
Pt(111)	1.62	Nat. Catal., 2018, 1, 339-348
Fe-Pc	1.88	Nanoscale, 2015, 7, 11633-11641
PtTe	1.89	J. Am. Chem. Soc. 2018, 140, 12732-12735
Fe-pyridine-N_4-C	1.90	Nat. Catal., 2018, 1, 339-348
Co-pyridine-N_4-C	2.59	Nat. Catal., 2018, 1, 339-348
Fe-pyrrole-N_4-C	2.05	Nat. Catal., 2018, 1, 339-348
Tc-pyrrole-N_4-C	1.73	Nat. Catal., 2018, 1, 339-348
Os-pyrrole-N_4-C	2.31	Nat. Catal., 2018, 1, 339-348

Table S7. Bond length of metal-oxygen *l*(M-O) (Å) and activated O-O *l*(O-O) (Å) of O_2 molecule adsorption on M-Ti_2CO_2 (M = 3d transition-metal) active sites.

system	l_{M-O}	l_{O-O}
Ti-Ti_2CO_2	1.82	1.46
V-Ti_2CO_2	1.79	1.45
Cr-Ti_2CO_2	1.77	1.43
Mn-Ti_2CO_2	1.84	1.40
Fe-Ti_2CO_2	1.71	1.27
Co-Ti_2CO_2	1.76	1.27
Ni-Ti_2CO_2	1.82	1.28
Cu-Ti_2CO_2	1.86	1.28

Table S8. Adsorption free energy of OH (ΔG_{*OH}, eV), O (ΔG_{O*}, eV), OOH (ΔG_{*OOH}, eV) and reaction free energy (ΔG_1, ΔG_2, ΔG_3 and ΔG_4, eV vs. RHE) of elementary step as well as overpotential (η, V) for ORR at U_{RHE} = 0 V proceeded on M-MXenes (M = Cu, Pd, Ag, Pt and Au).

Active center	ΔG_{*OOH}	ΔG_{O*}	ΔG_{*OH}	ΔG_1	ΔG_2	ΔG_3	ΔG_4	η
Ideal	3.69	2.46	1.23	-1.23	-1.23	-1.23	-1.23	0
Pt/C[5]	-	-	-	-	-	-	-	0.40
Pt(111)[1]	4.10	1.62	0.80	-0.82	-2.48	-0.82	-0.80	0.43
Cu-Ti_2CO_2	3.76	2.78	1.25	-1.16	-0.98	-1.53	-1.25	0.25
Pd-Ti_2CO_2	4.05	2.80	1.81	-0.87	-1.25	-0.99	-1.81	0.36
Ag-Ti_2CO_2	4.37	3.60	1.79	-0.55	-0.78	-1.81	-1.79	0.68
Pt-Ti_2CO_2	3.28	1.53	1.26	-1.64	-1.75	-0.27	-1.26	0.96
Au-Ti_2CO_2	3.14	2.69	1.68	-1.78	-0.45	-1.01	-1.68	0.78
Cu-$Ti_3C_2O_2$	3.72	2.79	1.42	-1.20	-0.93	-1.37	-1.42	0.30
Pd-$Ti_3C_2O_2$	3.91	2.59	1.95	-1.01	-1.32	-0.64	-1.95	0.59
Ag-$Ti_3C_2O_2$	4.34	3.79	2.00	-0.58	-0.54	-1.79	-2.00	0.69
Pt-$Ti_3C_2O_2$	3.04	1.44	0.94	-1.88	-1.61	-0.49	-0.94	0.74
Au-$Ti_3C_2O_2$	3.12	2.69	1.71	-1.80	-0.43	-0.97	-1.71	0.80
Cu-Ti_3CNO_2	3.76	2.81	1.30	-1.16	-0.95	-1.51	-1.30	0.28
Pd-Ti_3CNO_2	3.81	2.50	1.64	-1.11	-1.31	-0.87	-1.64	0.36
Ag-Ti_3CNO_2	4.50	3.76	1.96	-0.42	-0.74	-1.80	-1.96	0.81
Pt-Ti_3CNO_2	2.88	1.33	0.81	-2.04	-1.55	-0.51	-0.81	0.72
Au-Ti_3CNO_2	3.17	2.66	1.70	-1.75	-0.52	-0.96	-1.70	0.71

Table S9. Binding energies (E_b, eV) of H_2O, CO and O_2 adsorption, wherein H_2O-Cu-Ti_2CO_2 (CO-Cu-Ti_2CO_2) means that H_2O (CO) is first adsorbed, and then the substrate continues to adsorb another molecule.

system	adsorbed molecule	E_b
Cu-Ti_2CO_2	O_2	-0.79
	H_2O	-0.82
	CO	-1.55
H_2O-Cu-Ti_2CO_2	O_2	-0.35
CO-Cu-Ti_2CO_2	O_2	0.06
O_2-Cu-Ti_2CO_2	O_2	-0.05
	H_2O	-0.37
	CO	-0.69

Table S10. Total energy of a metal atom in the bulk with the most stable crystal phase (μ_M , eV/atom) and a single metal atom in the vacuum (E_M^{single} , eV/atom), as well as the metal cohesive energy ($E_{coh} = \mu_M - E_M^{single}$, eV/atom). The values of E_{coh} are compared to the available PBE results and experimental values taken from Ref. [6].

Metals	Crystal phases	E_M^{bulk}	E_M^{single}	E_{coh}	PBE	Exp.
Ti	hcp	-7.80	-2.42	-5.38	-	-
V	bcc	-8.96	-3.56	-5.40	-	-
Cr	bcc	-9.51	-5.43	-4.08	-	-
Mn	bcc	-8.85	-5.16	-3.69	-	-
Fe	bcc	-8.25	-3.25	-5.00	-	-
Co	hcp	-7.03	-1.72	-5.31	-	-
Ni	fcc	-5.49	-0.65	-4.84	-	-
Cu	fcc	-3.83	-0.24	-3.59	-3.48	-3.52
Zr	hcp	-8.52	-2.28	-6.24	-	-
Nb	bcc	-10.09	-3.15	-6.94	-	-
Mo	bcc	-10.92	-4.61	-6.31	-	-
Tc	hcp	-10.35	-3.31	-7.04	-	-
Ru	hcp	-9.23	-1.50	-7.73	-	-
Rh	fcc	-7.26	-1.24	-6.02	-5.72	-5.78
Pd	fcc	-5.21	-1.50	-3.71	-3.71	-3.92
Ag	fcc	-2.70	-0.20	-2.50	-2.52	-2.97
Hf	hcp	-9.93	-3.52	-6.41	-	-
Ta	bcc	-11.81	-3.58	-8.23	-	-
W	bcc	-13.02	-4.54	-8.48	-	-
Re	hcp	-12.39	-4.64	-7.75	-	-
Os	hcp	-11.23	-2.93	-8.30	-	-
Ir	fcc	-8.84	-1.51	-7.33	-	-
Pt	fcc	-6.09	-0.53	-5.56	-	-
Au	fcc	-3.21	-0.19	-3.02	-	-

Table S11. Diffusion barrier of Ti, V, Fe, Co, Ni and Cu single-atoms on Ti_2CO_2 surface.

system	diffusion barrier (eV)
Ti-Ti_2CO_2	1.43
V-Ti_2CO_2	1.15
Fe-Ti_2CO_2	0.86
Co-Ti_2CO_2	0.70
Ni-Ti_2CO_2	0.75

Cu-Ti_2CO_2	0.25

Figures

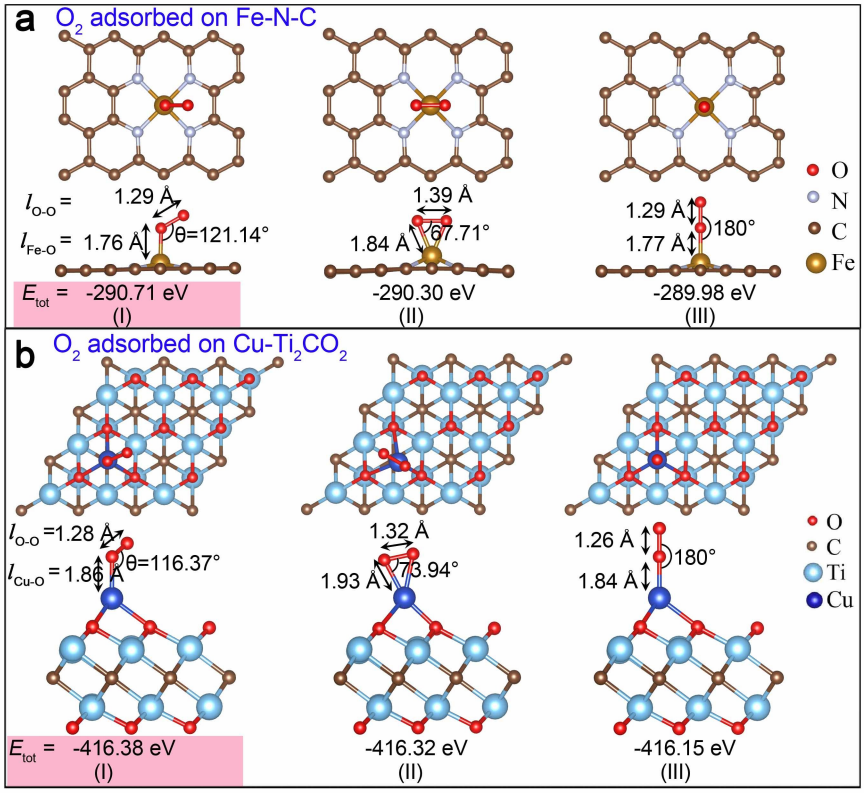

Fig. S1 Configuration test for O_2 adsorbed on the active sites of (a) Fe-N-C and (b) Cu-Ti_2CO_2, where the optimized total energy (E_{tot}), the bond length and the bond angle are highlighted. The optimal adsorption configuration is marked with pink.

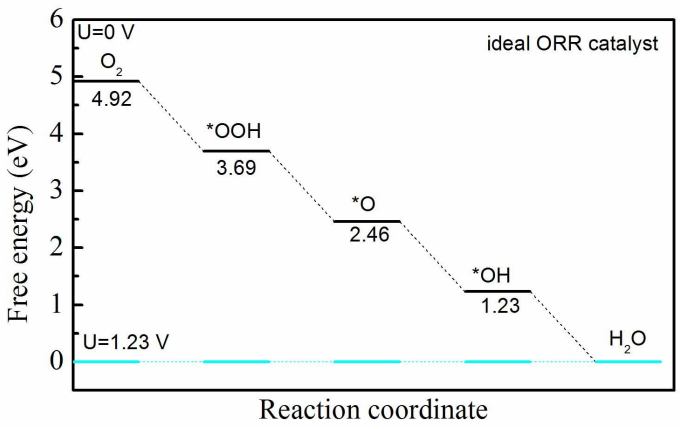

Fig. S2 Free energy profile of the ORR proceeded on an ideal catalyst at zero electrode potential.

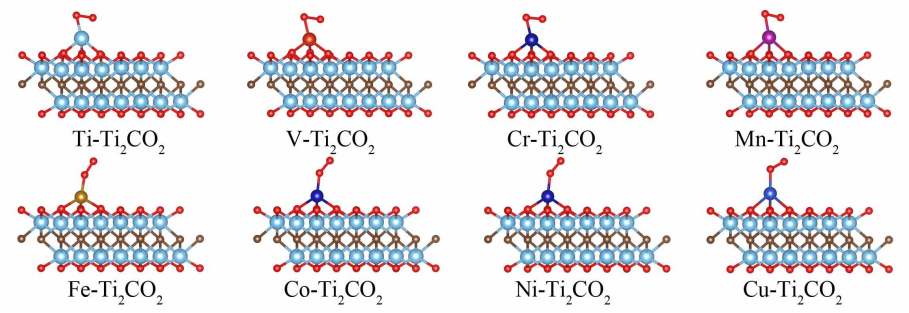

Fig. S3 The optimized configurations of O_2 molecule adsorption on Ti, V, Cr, Mn, Fe, Co, Ni, Cu anchored Ti_2CO_2.

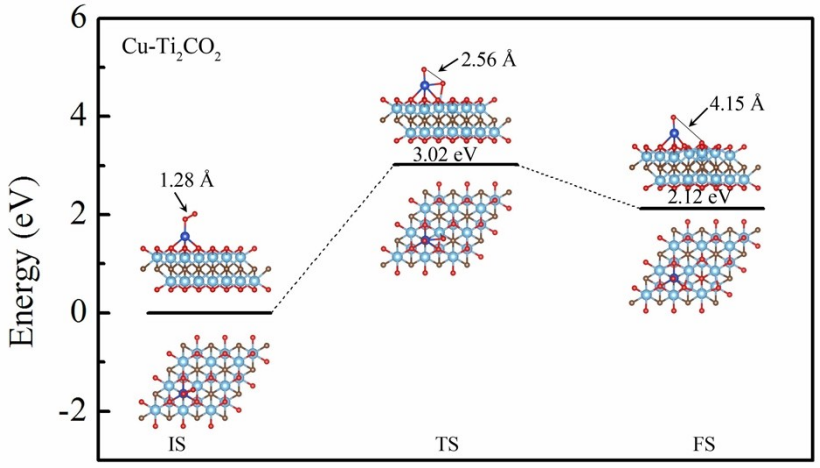

Fig. S4 Energy profile for the O_2 dissociation reaction on the surface of Cu-Ti_2CO_2. The IS, TS, and FS represents initial state, transition state, and final state, respectively.

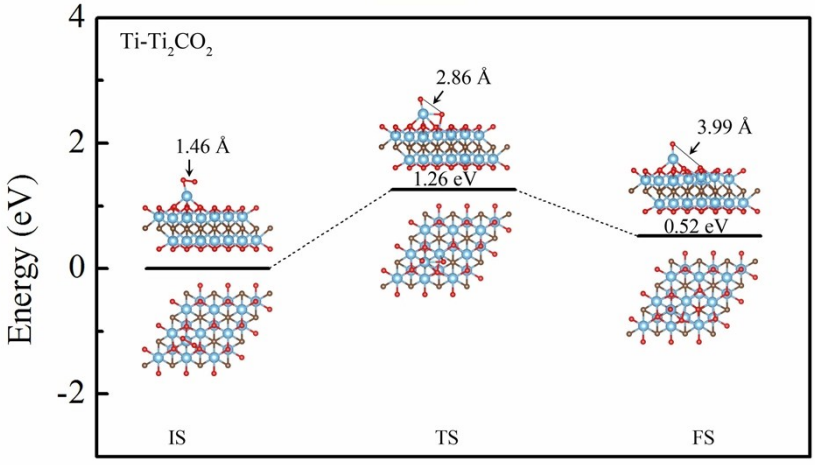

Fig. S5 Energy profile for the O_2 dissociation reaction on the surface of Ti-Ti_2CO_2. The IS, TS, and FS represents initial state, transition state, and final state, respectively.

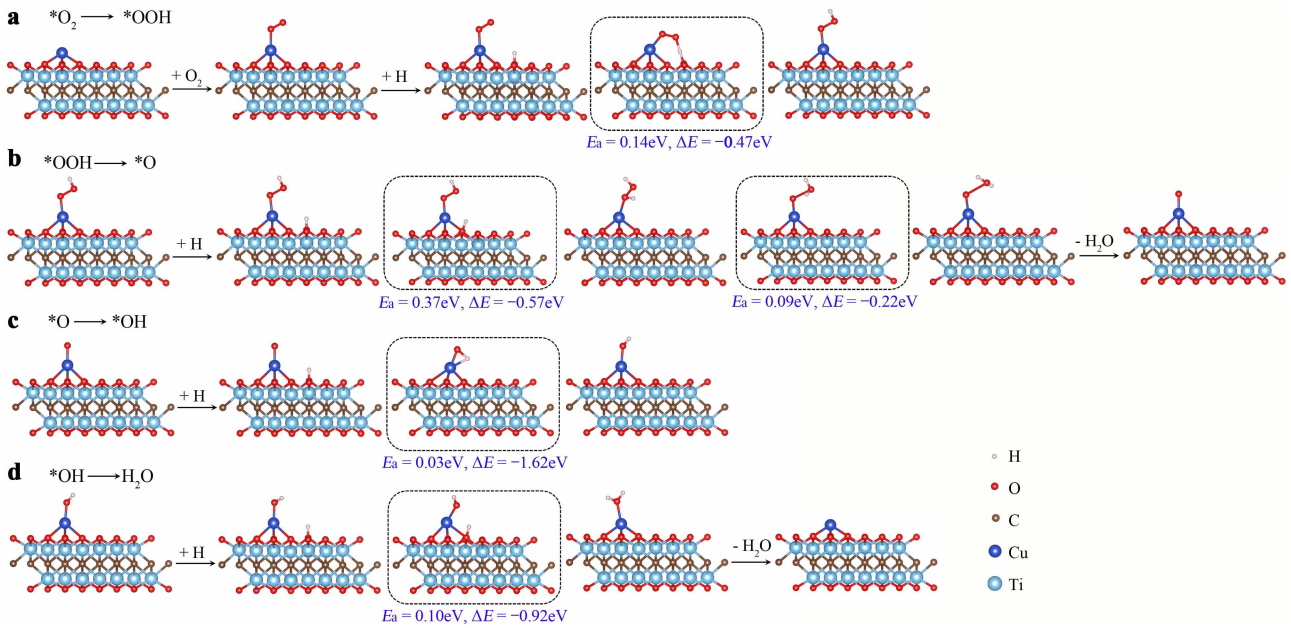

Fig. S6 Schematic of four elementary steps: (a) *OOH formation from the hydrogenation of the adsorbed O_2 on Cu-Ti_2CO_2. (b) 1st H_2O formation from the hydrogenation of *OOH, then H_2O release to form O*. (c) *OH formation from the hydrogenation of O*. (d) 2nd H_2O formation from the hydrogenation of *OH, then H_2O release to restore Cu site. The transition state is marked with a rectangular frame. The corresponding activation energy barrier (E_a) and reaction energy (ΔE, total energy change between product and reactant) are shown below the rectangular frame.

High selectivity for 4*e* oxygen reduction

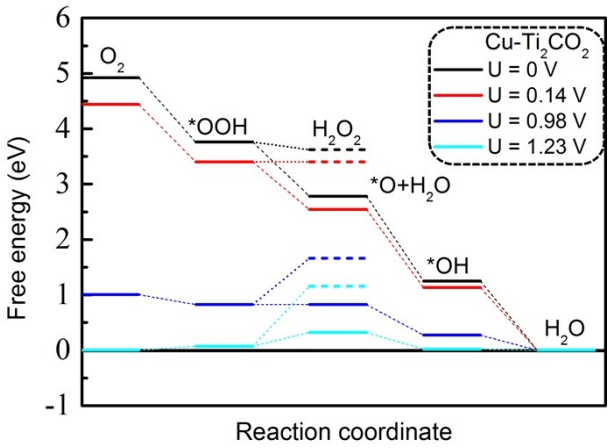

Fig. S7 Free energy profile of 4*e* and 2*e* ORR proceeded on Cu-Ti_2CO_2. Starting from the formation of *OOH intermediate, the solid and dotted lines represent the 4*e* and 2*e* reduction pathways, respectively.

In acidic media, the competitive side reaction of 4*e* ORR is the 2*e* reduction process, in which the O_2 is reduced to H_2O_2. Due to the formation of *OOH species, it can be further hydrogenated by reacting with another proton. This step can be written as:

$$*OOH + H^+ + e^- \rightarrow H_2O_2 .$$

As shown in Fig. S7, although the 2*e* process on Cu-Ti_2CO_2 is downhill in the free energy diagram at zero potential (U_{RHE} = 0), the step from *OOH to H_2O_2 will turn to be uphill upon the potential higher than 0.14 V. In this case, the 2*e* reduction pathway is unfavorable. In contrast, at 0.14 < U < 0.98 V, all the intermediate steps of 4*e* reduction process are still downhill in the free energy profile, which is exothermic and energetically favorable. Therefore, the Cu-Ti_2CO_2 catalyst has high selectivity for the 4*e* reduction pathway in which O_2 is reduced to H_2O.

Effects of H_2O, CO or multiple O_2 adsorption on the catalytic performance of Cu site

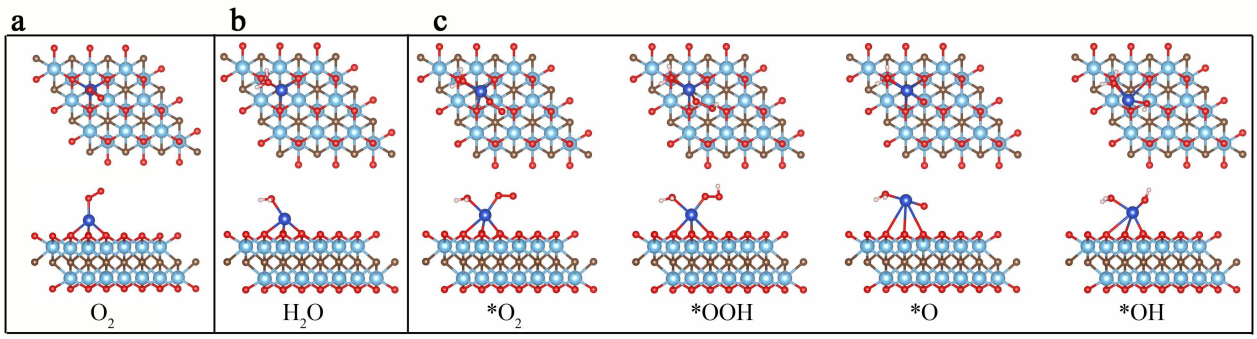

Fig. S8 Optimized atomic structures of (a) O_2 and (b) H_2O molecules adsorbed on the active site of Cu-Ti_2CO_2. (c) Optimized atomic structures of ORR intermediates on H_2O attached Cu-Ti_2CO_2.

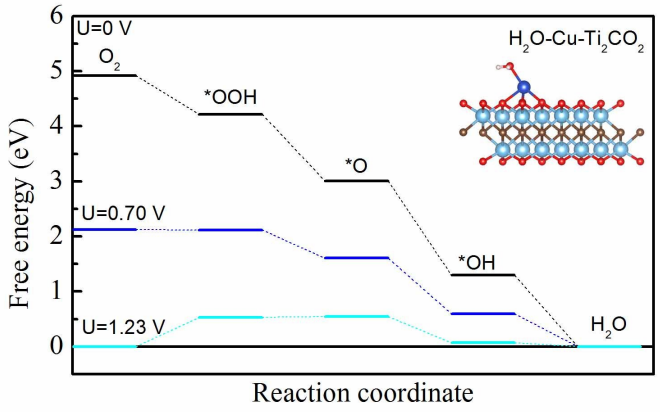

Fig. S9 Free energy profile of the ORR proceeded on H_2O-Cu-Ti_2CO_2.

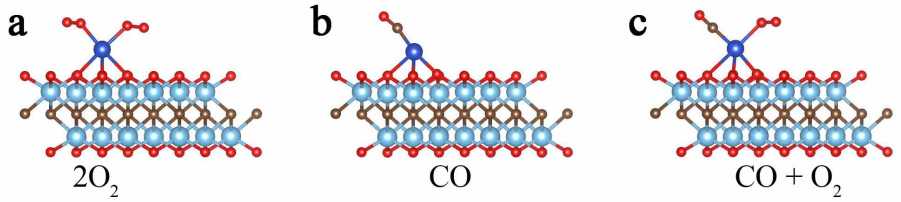

Fig. S10 Optimized atomic structures of (a) two O_2 molecules, (b) one CO molecule as well as (c) CO and O_2 molecules adsorbed on the active site of Cu-Ti_2CO_2.

The calculation of formation energy using the metal bulk energy

In addition, the formation energy E_f of metal atom anchored MXenes is calculated using the metal bulk energy, which is given by the following expression,

$$E_f = E_{M\text{-}MXenes} - E_{MXenes} - \mu_M , \quad (13)$$

where $E_{M\text{-}MXenes}$ and E_{MXenes} are the total energies of the whole system and free MXenes, respectively, and μ_M is the chemical potential of metal, i.e., the total energy of metal atom in the bulk with the most stable crystal phase, as summarized in Table S10. For comparison, the formation energies E_f of M-N-C SACs are also calculated according to equation 14, because they have been synthesized and considered as promising ORR catalysts to replace Pt/C, where M-N-C refers to the metal (M) (such as Fe, Co, Ni and Cu) and nitrogen (N) co-doped on the graphene support (C).

$$E_f = E_{M\text{-}C\text{-}N} - \sum_x n_x \mu_x , \quad (14)$$

where $E_{M\text{-}C\text{-}N}$ is the total energy of M-C-N whole system, and n_x is the number of M, N and C atoms. The corresponding chemical potentials μ_x are derived from the metal bulk, gaseous N_2 (-8.31 eV/atom) and graphene (-9.21 eV/atom), respectively. As seen in Fig. S11, the formation energy E_f of Cu-Ti_2CO_2 is 1.95 eV. Although the E_f value is positive, it is comparable to that of the experimentally available Fe-N-C (1.19 eV) and Cu-N-C (1.95 eV) SACs. This indicates that they have comparable stability, further confirming the thermodynamic stability of Cu-Ti_2CO_2.

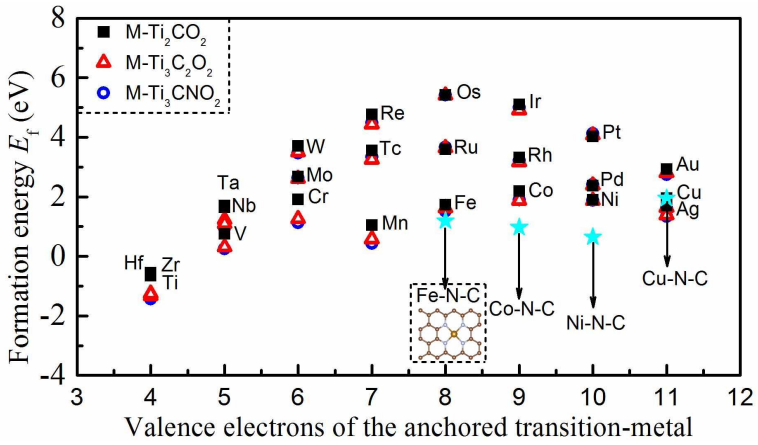

Fig. S11 Formation energy of metal atom M (M = 3d, 4d and 5d transition-metal) anchored on the surface of Ti_2CO_2, $Ti_3C_2O_2$ and Ti_3CNO_2 (labeled as M-Ti_2CO_2, M-$Ti_3C_2O_2$ and M-Ti_3CNO_2).

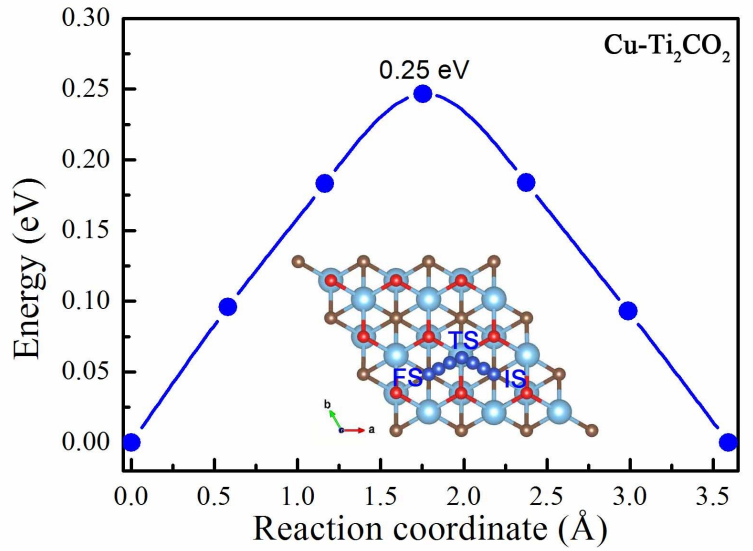

Fig. S12 Diffusion barrier of Cu atom on the surface of Ti_2CO_2, where the IS, TS and FS represent the initial state (at the hollow site between three neighboring O atoms and on the top site of C atom), transition state (at the top site of Ti) and final state (at the hollow site between three neighboring O atoms and on the top site of C atom), respectively.

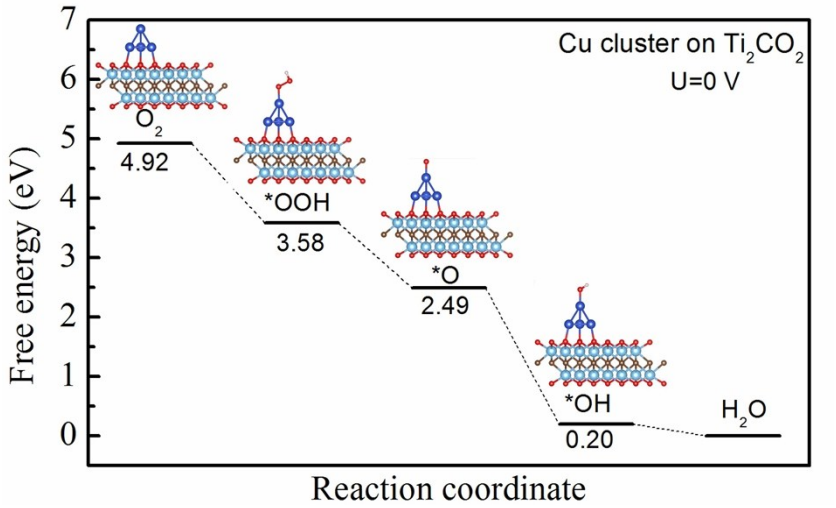

Fig. S13 Free energy profile of the ORR proceeded on Cu4-Ti_2CO_2 and the optimized atomic structures of reaction intermediates (*OOH, O* and *OH). Cu4 corresponds to face-centered cubic Cu with 4 atoms.

References

1. J. K. Nørskov, J. Rossmeisl, A. Logadottir, L. Lindqvist, J. R. Kitchin, T. Bligaard and H. Jónsson, *J. Phys. Chem. B*, 2004, **108**, 17886-17892.
2. H. Xu, D. Cheng, D. Cao and X. C. Zeng, *Nat. Catal.*, 2018, **1**, 339-348.
3. D. R. Stull and H. Prophet, *JANAF thermochemical tables*, U.S. National Bureau of Standards, Washington, DC, 1971.
4. J. Rossmeisl, Z. W. Qu, H. Zhu, G. J. Kroes and J. K. Nørskov, *J. Electroanal. Chem.*, 2007, **607**, 83-89.
5. Y. Chen, S. Ji, S. Zhao, W. Chen, J. Dong, W.-C. Cheong, R. Shen, X. Wen, L. Zheng, A. I. Rykov, S. Cai, H. Tang, Z. Zhuang, C. Chen, Q. Peng, D. Wang and Y. Li, *Nat. Commun.*, 2018, **9**, 5422.
6. G. I. Csonka, J. P. Perdew, A. Ruzsinszky, P. H. T. Philipsen, S. Lebègue, J. Paier, O. A. Vydrov and J. G. Ángyán, *Phys. Rev. B*, 2009, **79**, 155107.